DOI: https://doi.org/10.36094/sc.v89.2025.Thermal_Barrier_Coatings_for_Aerospace.Aruna_Kumar.62

ARTICLE

Sci. and Cult. 91 (1–2) : 62-72 (2025)

THERMAL BARRIER COATINGS FOR AEROSPACE INDUSTRY: A MINI REVIEW

S.T. ARUNA* AND S. SENTHIL KUMAR#

Thermal barrier coatings (TBCs) are highly advanced high-temperature coatings applied to superalloy surfaces of gas turbine or aero-engine parts that operate at very high temperatures. TBCs are indispensable for aerospace industry and the operational efficiencies of GT engines are enhanced with TBCs. This mini review article details the need for TBCs, the history of TBCs, the various components of TBCs, the materials used, the challenges faced by TBCs and the recent trends in TBCs. It also highlights the significant TBC research carried out at CSIR-National Aerospace Laboratories (NAL).

Keywords: *Gas turbine; TBCs; bond coat, topcoat; plasma spray; hot corrosion; CMAS*

Introduction

Gas turbine (GT) engines aid in aircraft electric propulsion and also electricity generation and they are responsible for taking us skywards[1-5]. They generate the thrust required to propel aircraft through the air. To generate electricity, the GT heats a mixture of air and fuel at very high temperatures, resulting in the spinning of turbine blades that in turn drives a generator which converts the energy into electricity (Fig.1). GTs are also used in land based industrial GTs and marine turbines. There is an interest in increasing the operational efficiency of the aircraft engines by increasing the operating temperatures as the performance is intrinsically related to the GT inlet temperature. With high operating temperatures, the bare nickel-based superalloy engine components attain melting temperatures resulting in the failure of the components. Further, coatings are indispensable to GT components made of superalloys due to the following reasons: (i) Severe ingress of sulphur takes place into the material leading to the formation of metal sulphides that further leads to decrease in mechanical properties of the materials resulting in disastrous failures, (ii) Development of an alloy possessing synergistic combination of high-temperature strength and hot-corrosion resistance is challenging, (iii) The addition of W, Mo and V to superalloys assists in enhancing the high temperature strength. However, superalloys are highly vulnerable to hot corrosion in presence of these elements.

The efficiency of the GT depends on the gas entry temperature. By increasing the gas inlet temperature, the efficiency and electricity output increases, which in turn improves the thrust to weight ratio and reduces CO_2 emissions. However, the GT components cannot withstand these higher temperatures. Thus there is a need to protect the GT components from high temperatures by using thermal barrier coatings [5-13].

Currently, all the GT components are coated with thermal barrier coatings (TBC) for protecting the structural engine components from degradation at severe high operating temperatures in the range of 1300 to 1500°C (Fig.2). TBCs provide insulation to metallic components from extended heat loads. They help in the increased

* Surface Engineering Division, CSIR-National Aerospace Laboratories, Bengaluru 560017, India

Corresponding Author: aruna_reddy@nal.res.in

e-mail: ssenthil@nal.res.in

lifetime of components by decreasing oxidation and thermal fatigue. TBCs facilitate flame temperatures more than the melting point of the metal airfoil. Initially, Ni-based alloys could be used at~1000°C. After the introduction of convectional cooling, they could be operated close to 1100°C. With the advent of TBCs, Ni-based alloys could be used up to 1300°C and with the advanced TBC and film cooling, GTs can be operated close to 1500°C. Nevertheless, the life of TBCs will be reduced due to different types of degradations. The rapid development of the aviation industry has put forward increasingly higher demands for aero-engines with large thrust, high efficiency, and low fuel consumption, becoming the general objectives of engine design and manufacturing. TBCs act as thermal insulation layers and protect the underlying superalloy substrates from the severe environment by bringing down the components' surface temperatures by 100-300°C depending on the thermal conductivity, thickness and microstructure of the ceramic topcoat. TBC brings down the metal temperature and enhances the life of GT components by stopping oxidation and creep damage. Recent studies have also shown that the increased Turbine Entry Temperature (TET) and TBCs will reduce the carbon foot-print. A study has shown that by using TBC technology on a single aircraft, there was a reduction in carbon emissions by~1100 MT/yr. The TBCs facilitate the increase in TET which in turn increases the thermal efficiency. It helps to decrease the CO and NOx emissions and 15-20% decrease in fuel consumption and 8% increase in engine power[14]. More details on

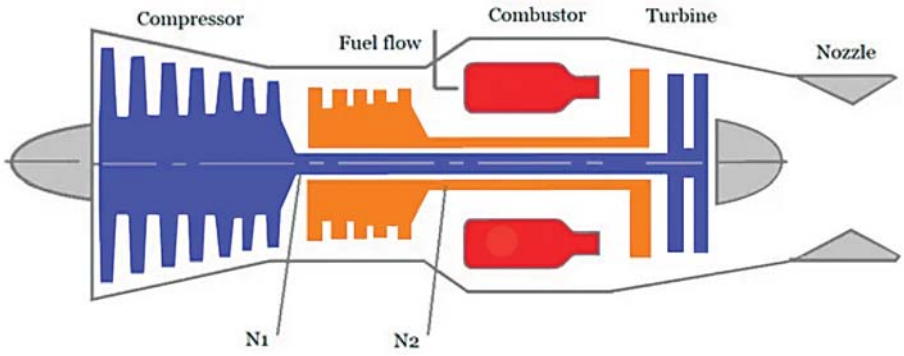

Fig. 1: Schematic of a gas turbine engine (adapted from https://www.mdpi.com/2075-1702/9/3/49)

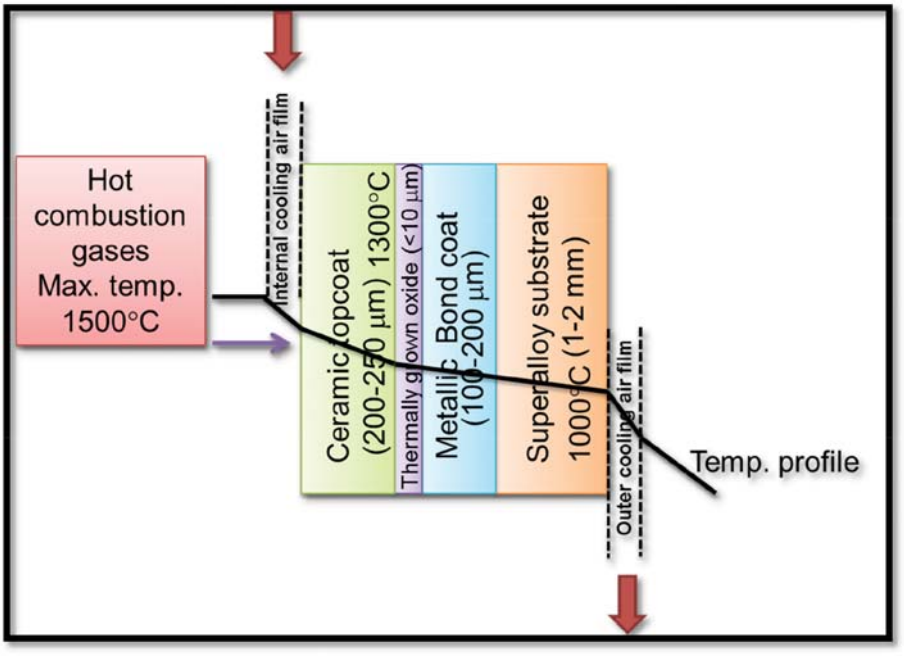

Fig. 2: Schematic showing the cross-section of a thermal barrier coating along with the temperature profile.

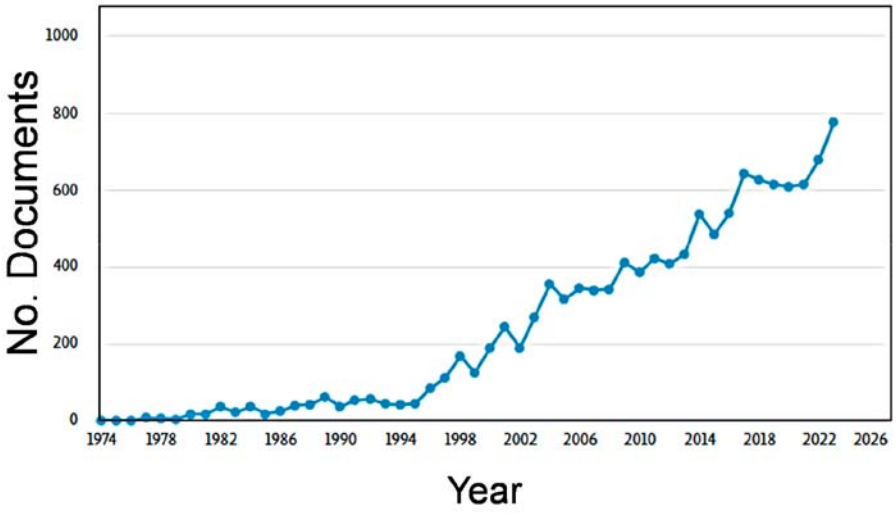

Fig. 3: Plot showing the number of publications on TBCs globally (As per the Scopus database accessed on 23/02/2023).

TBCs can be obtained from a large number of review articles published on various aspects of TBCs[1-14].

History of TBCs

TBCs have a long history as evident from the NASA report[15]. During 1942-1956, National Advisory Committee for Aeronautics (NACA) developed NBS frit enamel coatings.This was the first aero ceramic coatings paper that was published in 1947[16]. In 1948, the NBS frit coating was deposited on turbine blades in an engine and tested[17]. Also, American Air Force developed frit coatings in the 1940s, 50s and 60s[18]. In 1960 for the first time, Rokide™ TBC was applied on XLR99 rocket engine nozzles of the X-15 using flame spray process. Nickel chrome bond coat and zirconia topcoat were sprayed mainly to prevent the oxidation of brazed stainless steel tube structures through which liquid ammonia was circulated. TBC also helped in preventing the boiling of liquid ammonia[19]. In 1950s TBCs played a crucial step towards liquid hydrogen (LH_2)/liquid oxygen (LOX) rocket development. In 1961, Sal Grisaffe conducted basic thermal spray research in 1960s. In the early 1970s, Al_2O_3, CaO and Y_2O_3 stabilized ZrO_2 and HfO_2 coatings were developed for nuclear rocket applications [20, 21]. Meanwhile TBCs were used in low risk aero applications by Pratt & Whitney (P&W). By 1970, plasma sprayed TBC were in vogue in commercial combustors[22].

In mid 70s, modern TBCs containing zirconia-12%yttria ceramic topcoat on NiCrAlY bond coat were developed and the coating survived the J-75 engine test. The key accomplishments of this study were the use of (i) yttria as stabilizer for zirconia, (ii) use of MCrAlY type bond coat and (iii) first demonstration of TBC on blade[23]. In 1977, the NASA TBC was tested with heterogeneous results in a more advanced JT9D at P & W wherein the coating spalled in high temperature regions and it was intact in lower temperature regions[24].

In 1978, Stecura reported optimum zirconia-yttria TBC composition of ~6wt% . He evaluated the thermal cycling ability of TBCs containing different wt% of yttria and he found that 7wt% yttria stabilized zirconia exhibited ~70 more thermal cycles than 8wt% YSZ[25]. A later work of Stecura showed two times higher life for TBC with YbSZ and a Yb-containing bond coat[26].

NASA sponsored P & W research efforts and recognized 3 optimum 6YSZ TBC microstructures containing conventional plasma sprayed YSZ, segmented plasma sprayed TBC and EB-PVD TBC. The coatings were subjected to 4 min burner rig cycles at 1079°C and EB-PVD coating sustained >8000 cycles and segmented TBC close to 8000 cycles and conventional YSZ coating withstood only 7000 cycles[27]. Paul Siemens of GE recognized the significance of bond coat oxidation and plasticity[28].

In the 1980s NASA efforts continued on TBCs and TBC creep studies were initiated and studies on calcium magnesium alumino silicate (CMAS) attack and hot corrosion studies were discussed [29,30]. NASA continued its efforts on improving TBCs. Industry trials were taken up and many different applications were explored. TBCs were used in 2 major NASA projects with GE and P & W and the value of TBCs was analytically assessed. In 1985, P & W employed YSZ TBC to address a vane platform endurance problem and the studies showed elimination of distress of vane platform and extended service life to 18,000 hours[31]. Many institutes and companies initiated the TBC life prediction studies[32]. TBC life model development studies were also initiated by NASA, GE, P & W, etc. Efforts were also made in understanding various failure mechanisms.

As per the grand view market survey, "the global thermal barrier coatings market size was valued at USD 16.1 billion in 2022 and is expected to grow at a compounded annual growth rate (CAGR) of 5.1% from 2023 to 2030". As per the survey, the TBC market by materials shows a maximum share for ceramic yttria stabilized zirconia followed by alumina and MCrAlY. The key companies that are currently operating in the thermal barrier coatings market include: Oerlikon Metco, Metallization Ltd., Praxair Surface Technologies Inc., Metallizing equipment Co. Pvt. Ltd., ASB Industries, Thermion Inc., HC Stack Inc., The Fisher-Barton Group, etc.

To analyze the research trends in TBCs, scopus analysis was carried out using the search words: thermal barrier coatings and thermal barrier coatings+India (Fig. 3 to Fig. 7). It is clearly evident from the papers published on thermal barrier coatings clearly an increased interest in the TBCs research. Among countries, China tops the list followed by USA, Germany, Japan and India. Among the various research institutes involved in the TBC research in India, DMRL tops the list followed by Anna University, IIT Bombay, IISc, etc. In this review article, more details about the structure, materials, recent trends and work carried out at CSIR-NAL will be discussed.

Structure of the TBC System

The schematic of the cross-section of a typical TBC system is depicted in Fig.2. It consists of a 1-2 mm thick superalloy substrate. The CTE of Ni superalloy is $16x10^{-6}$

K^{-1} and over this the bondcoat material (100-200 µm) with a CTE of 17.5 x 10^{-6} K^{-1} is deposited. Over the bond coat, a ceramic topcoat with a thickness of 200-250 µm is deposited. More details about all these components are provided below.

Substrate: Nickel or cobalt based superalloys (1-4 mm thickness) are used as the substrate material in GTs due to their high specific strength at high temperatures. They possess good mechanical properties along with corrosion and oxidation resistance. However, they are susceptible to creep and cyclic fatigue. The internal surfaces of superalloy components are cooled with air. The Ni-based superalloys are most widely used substrates and they possess a thermal expansion coefficient (TEC) close to 16 × 10^{-6} K^{-1}.

Bond Coat Materials: The bond coat is deposited using plasma spray or HVOF technique. MCrAlY is the latest generation bond coat material; it does not interact with the substrate. During plasma spraying secondary aluminum oxide is formed. The bond coat forms an outer layer of chromia and an alumina layer underneath. Usually, the thermally grown oxide is formed when it is exposed to high temperatures. The chromia provides oxidation and hot-corrosion resistance. Alumina forms a self-passivating layer and controls further oxidation. The Y element present in MCrAlY assists in enhancing the adherence of the oxide to the substrate and limits the grain boundary growth. The other bondcoat materials are aluminides, Pt aluminides and cobalt cermets.

The bond coat is fabricated by low-pressure plasma spray

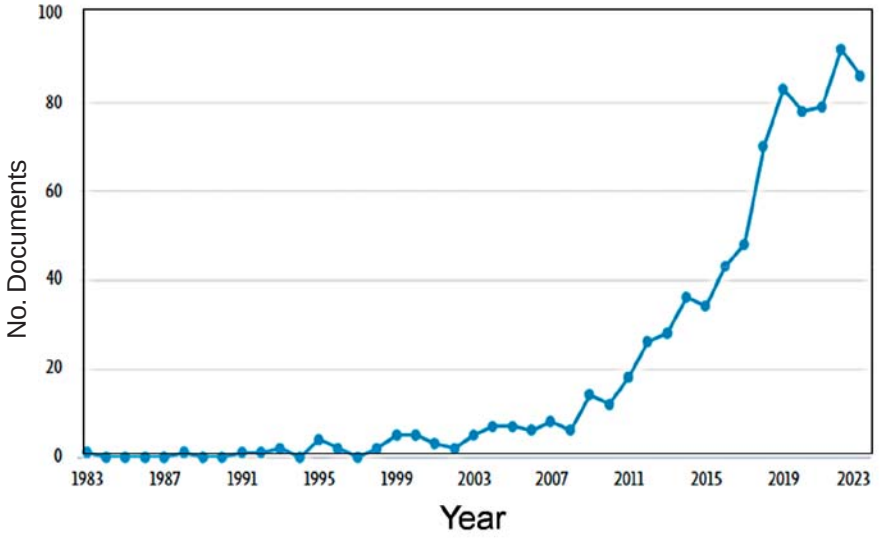

Fig. 4: Plot showing the number of publications on TBCs in India globally (As per the Scopus database accessed on 23/02/2023).

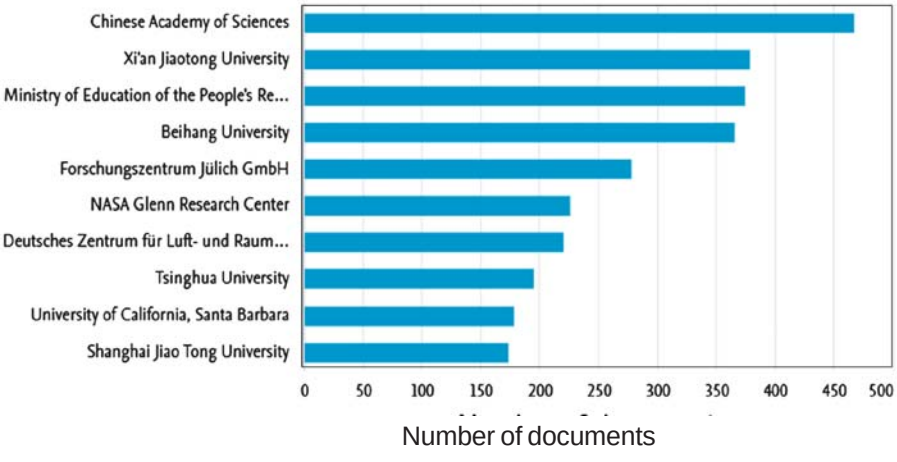

Fig. 5: Barchart showing the top research institutes publishing on TBCs globally) (As per the Scopus database accessed on 23/02/2023).

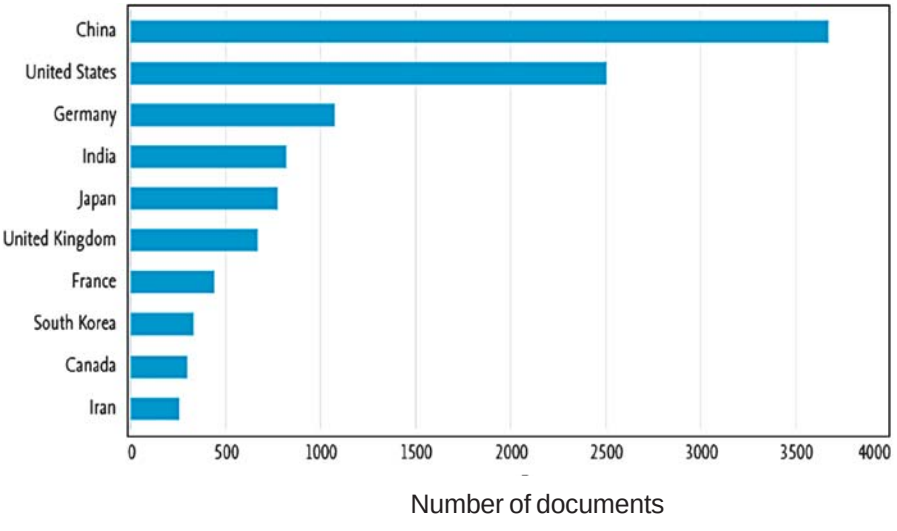

Fig. 6: Barchart showing the top research institutes publishing on TBCs globally (As per the Scopus database accessed on 23/02/2023).

(LPPS), APS and high-velocity oxy-fuel (HVOF). As these spray processes are line-of-sight methods, they require complex robotic manipulator for realizing uniform coating coverage. Further, the oxide content can be high in APS coatings. APS process also results in higher porosity compared to HVOF and LPPS processes. The other possible processes for bond coat are: (i) electrolytic codeposition, (ii) electrophoretic deposition and (iii) autocatalytic electroless deposition. The electrolytic codeposition or composite electroplating is a promising technique as it is a low cost process, non-line-of-sight process and it is able to produce homogeneous and dense coatings[33].

MCrAlY coatings have been successfully formed by this process. Ni-Al based coatings containing Al or Al_2O_3 particles have been developed by electrolytic co-deposition method. It is a two-step process wherein in the first step, Ni coating containing Al particles is developed by electrolytic codeposition. In the second step, a diffusion treatment is carried out during which Ni alloy coating containing Ni_3Al intermetallic phase is formed.

However, there is very scanty research on electrodeposited MCrAlY coatings. Such coatings have been developed by dispersing CrAlY powders in an electrolytic bath containing Ni, Co or Ni-Co. After codeposition, heat treatment has been carried out[34]. More details on this process can be obtained from the literature [35]. Dense MCrAlY coatings with a thickness of ~125 µm have been developed. This process has also been patented by Praxair which is known by the name Tribomet. This coating has been used as the abrasive tip coating on first stage turbine blades. Further, reports are limited and no systematic studies are available and the coatings have not been evaluated in syngas/hydrogen turbine environments.

Ceramic Topcoat Materials: The ceramic topcoat is a porous low thermal conductivity material. These materials have high strain compliance and the thickness varies for 200-250 µm. The important criteria for any material to be used as a TBC topcoat materials are as follows: (i) possess high melting point, (ii) they should not change their phase when they are cycled between room temperature and operation temperature, (iii) they should have low thermal conductivity, (iv) they should be chemically inert, (v) they should have matching coefficient of thermal expansion (CTE) with the metallic substrate, (vi) they should have good adhesion to the metallic substrate and (vii) the porous microstructure should undergo very low sntering rate. Partially stabilized tetragonal zirconia (t'-YSZ) is the most popular ceramic topcoat material as it possess a low thermal conductivity of ~2 W/mK, high thermal expansion coefficienct of 11×10^{-6} /K and it is chemically inert. The other promising materials for TBCs are $La_2Zr_2O_7$ and $La_2Ce_2O_7$ due to their lower thermal conductivity and close thermal expansion coefficient with 8YSZ (Table-1.).

Table 1. Properties of different TBC ceramic topcoat materials along with their properties

Material	Thermal Conductivity ($W\ m^{-1}K^{-1}$)	TEC (10^{-6}/K)
8YSZ	2	11
$La_2Zr_2O_7$	1.5	9
$La_2Ce_2O_7$	0.5	13

Thermally Grown Oxide (TGO): The thermally grown oxide (TGO) is formed near the topcoat and bond coat interface during service conditions. MCrAlY is the most widely used bond coat and the major oxide formed is alumina. Apart from that oxides with the composition Cr_2O_3, $(Cr, Al)_2O_3$, $Ni(Cr,Al)_2O_4$, NiO, SiO_2, etc are formed [36]. The TBC fails when the TGO thickness exceeds 10 µm thickness.

TBC Fabrication Methods

TBCs are generally fabricated using APS and EB-PVD techniques. APS is the most widely used technique for the fabrication of TBC. In this process, a plasma flame is generated by passing Argon/hydrogen gas mixture through a powerful electric arc discharge formed in the gap between two nonsacrificial electrodes like copper anode and tungsten cathode (Fig.8). High-temperature plasma (14000 K) is formed due to the heating up of the gas mixture by the released energy. The required powder is fed into the plasma jet at ~10000 K, the particles get melted and get deposited over the substrate placed at a suitable distance. The nature and properties of the coating is determined by factors such as plasma power, powder feed rate, standing distance, torch geometry, the nature of powders, etc. In the plasma spray process, high deposition rates are possible and is most widely used for the fabrication of TBCs. APS can be used to generate coatings of metals or a combination of metal and ceramics and the process results in the formation of a homogeneous coating having equiaxed grains. For the plasma spray applications, flowable powders are required. The plasma sprayable powders are prepared using techniques such as inert gas condensation, milling and crushing, milling and sintering, spray drying, cladding, RF-plasma spheroidization, etc (Fig.9).

Since EB-PVD TBCs have higher strain tolerance due to their columnar structure (Fig.10), the EB-PVD coatings are applied on moving parts of the TBCs and plasma sprayed coatings are applied on stationary parts. APS TBCs is mostly used for large and stationary aircraft engine components, such as nozzle guide vanes and combustor tiles or liners. Moreover, EB-PVD is utilized for the deposition of TBCs on rotary parts like high-pressure turbine blades[37]. APS coatings exhibit lower thermal conductivity due to the porous microstructure and presence of voids and cracks (Fig.10). The differences between the EB-PVD and APS developed TBCs are summarized in Table 2.

Evaluation Procedures of TBCs

It is very much essential to evaluate the mechanical, tribological and chemical properties of TBCs. Table-3 lists the various methods that are employed for evaluating the properties of TBCs. Apart from these, it is essential to evaluate the thermal conductivity of the coatings using the standard hot-disk and laser flash methods. Readers may refer the paper by Vaßen et al.[38] for better understanding the various methods used for evaluating the properties of TBCs. Further, simulating the realistic GT engine conditions to which the TBCs are subjected remains a big challenge.

Challenges with the State-of-the-art Ceramic Topcoat Material YSZ

Partially stabilized tetragonal zirconia is limited by its operation temperature of 1200°C. It

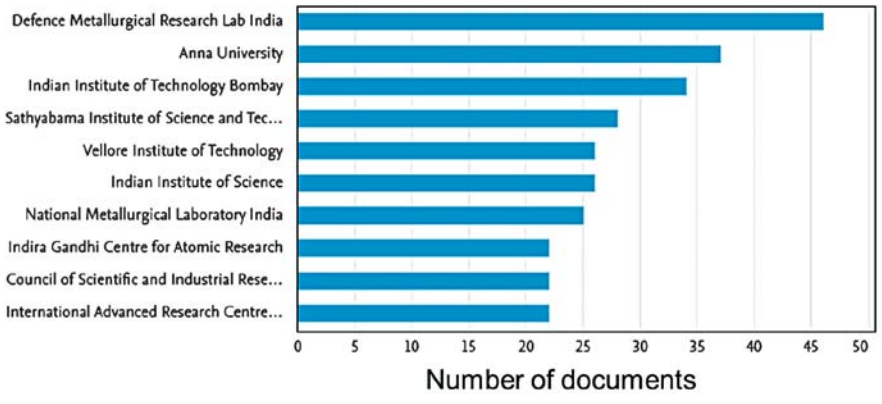

Fig. 7: Barchart showing the top research institutes publishing on TBCs in India (As per the Scopus database accessed on 23/02/2023).

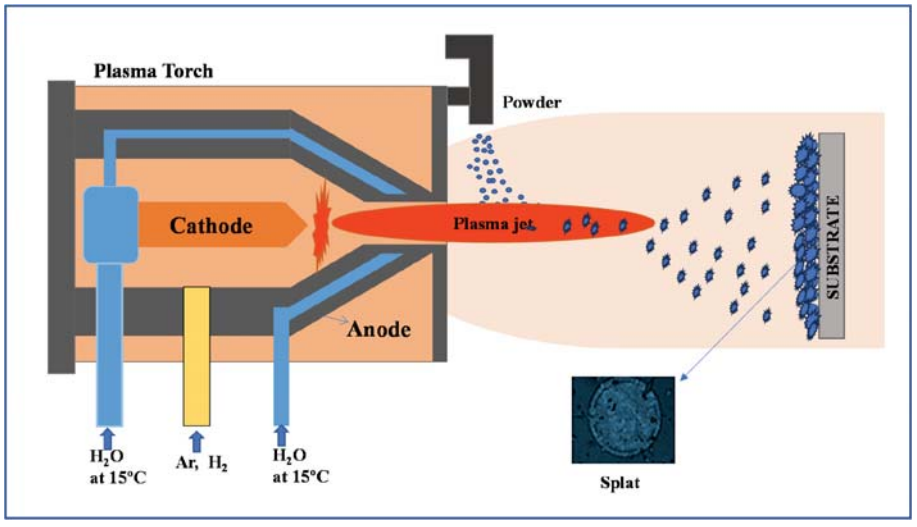

Fig. 8: Schematic of an atmospheric plasma spray system.

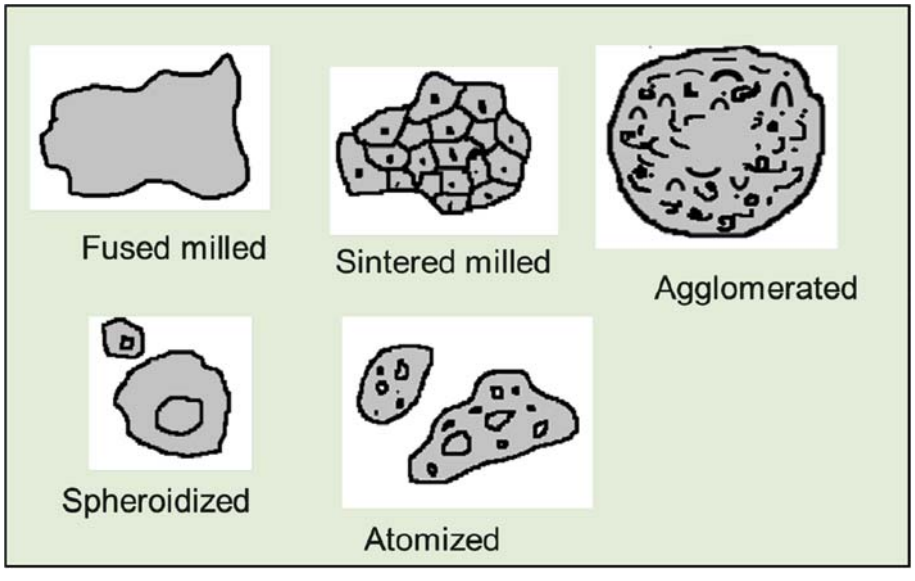

Fig. 9: Different shapes of sprayable powders employed for plasma spraying.

Table 2. Differences between EB-PVD and APS ceramic topcoat coatings.

S. no.	EB-PVD ceramic topcoat	APS ceramic topcoat
1.	It contain columnar grains	It containsplat grains
2.	Porous coating	Porous coating
3.	It has vertical cracks	It has horizontal cracks
4.	The coating possess high strain tolerance	The coating possess lower strain tolerance
5.	The coatings have longer spallation life	The coatings have shorter spallation life
6.	The coating has flat interface	The coating has rough interface
7.	The EB-PVD coatings are expensive; the capital investment is >20 million USD	The APS coatings are less expensive; the capital cost for APS is $2 million USD

Table 3. Evaluation procedures used for TBCs

Mechanical properties	Tribological properties	Chemical properties
• Tensile tests with and without adhesive • Shear test • Peel test • Scratch test • Ultrasonic test • Thermal wave ND scanning • Fracture toughness	• Adhesive wear test (ASTM C633-79) • Abrasive wear test • Long-term fatigue wear test • Erosive wear (ASTM G76-13)	• Burner rig test • Chemical corrosion evaluation test

undergoes phase transformation resulting in volume expansion and crack evolution. Sintering of YSZ above 1200°C results in catastrophic delamination. The YSZ is also susceptible to hot corrosion and calcium magnesium alumina silicate (CMAS) attack. Hence bi-layered and multi-layered YSZ/rare earth zirconates or cerate coatings are being explored.

TBC's Failure Mechanisms

Thermal cycling and mechanical loads can affect the TBC performance resulting in wear, cracks and topcoat delamination [39-43]. The chemical composition and topcoat microstructure can also result in failures. The thermal and mechanical response to operating conditions such as temperature, cycling time, combustion gases, also can cause failures. The oxidation of bondcoat is also one of the major causes for TBC failure. During cooling, the thermal expansion mismatch between TGO and bond coat will result in the residual compressive stresses. They attain a maximum at room temperature and may result in failure. Additionally, the compressive stresses generated during TGO growth cause TGO deformation and attribute to its undulated shape mostly under cycling conditions. During cycles, localized ingress in the bond coat progresses and downward displacements generate normal strains in TBC that spread laterally and finally coalesce giving rise to failure in one or both TGO interfaces and the phenomenon is referred to as ratcheting.

TBCs are also susceptible to hot corrosion [44,45]. Hot corrosion is a phenomenon which refers to the process of breakdown of protective oxide layers formed on metallic substrates. The breakdown happens due to the chemical interaction of the protective oxide film with definite aggressive species generated in the combustion environment and resulting in increased attack on the underlying metal. Hot corrosion occurs due to high concentrations of sulphur (~ 4 wt%), vanadium (~0.05 wt%) and sodium (~0.01 wt%) in the fuels. The S, V and Na impurities in the fuel undergo oxidation during combustion and form volatile compounds like SO_2, SO_3, NaOH, NaO, Na_2O, $VO(OH)_3$ and V_2O_4 that condense at 500-900°C and form deposits.

The type-I hot corrosion happens in the temperature range of 800 to 950°C. The molten Na_2SO_4 deposit is required to initiate hot corrosion attack. It is generally a thick and porous layer of oxides resulting in the depletion of chromium in the underlying alloy matrix followed by internal chromium-rich sulfides. The hot corrosion reactions that are prevalent with the state-of-the-art YSZ containing TBC are shown below:

(i) In the first step, V_2O_5 and Na_2SO_4 salt mixture reacts at a high temperature resulting in the formation of $NaVO_3$

$$V_2O_5 + Na_2SO_4 \rightarrow 2(NaVO_3) + SO_3$$

(ii) In the second step, $NaVO_3$ possessing a melting point of 610 °C, interacts with yttria from the YSZ solid solution to form YVO_4. As a result of this

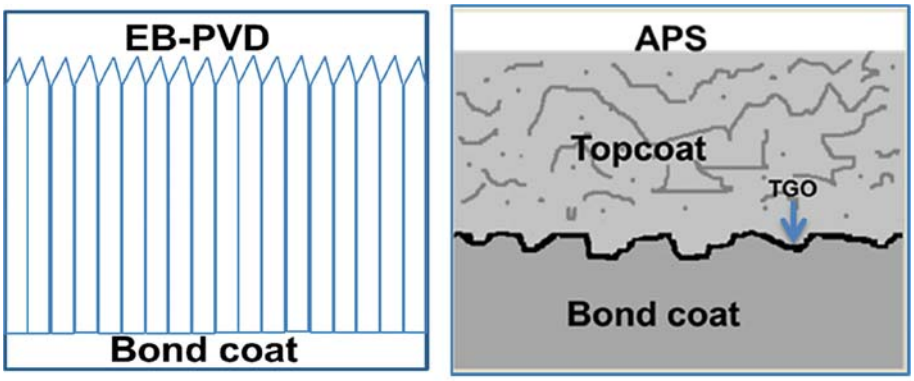

Fig. 10: Schematic showing the cross-section of TBC fabricated using EB-PVD and APS processes.

yttrium content gets depleted in the YSZ and hence results in the formation of monoclinic YSZ.

$$ZrO_2(Y_2O_3) + 2(NaVO_3) \rightarrow ZrO_2 + 2YVO_4 + Na_2O$$

(iii) Also Na_2O can react with V_2O_5 directly to form $NaVO_3$:

$$Na_2O(base) + V_2O_5(acid) = 2NaVO_3\ (salt)$$

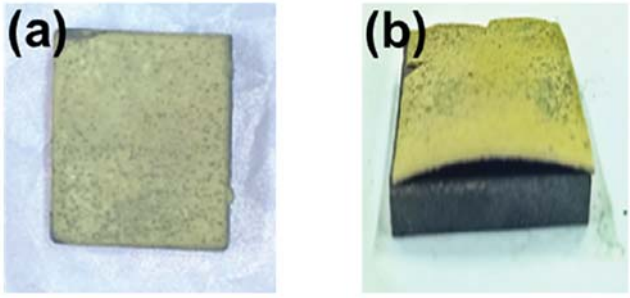

Fig. 11: Photograph of (a) in-house synthesized YSZ and (b) commercial YSZ TBCs that were exposed to high-temperature hot-corrosion.

Generally, for hot corrosion studies, a mixture of 45 wt% V_2O_5 and 55 wt% Na_2SO_4 is spread onto the surface of the coating by using a small spatula until a 25 mg/cm^2 salt concentration is obtained. The samples are placed in a muffle furnace and heated to 910°C in air environment for varying durations and once the samples are taken out from the furnace, the coating's microstructure and elemental composition are investigated. The coating subjected to hot corrosion is also characterized for phase identification using XRD. $Gd_2Zr_2O_7$ also reacts with molten salt to form $GdVO_4$ [45]. However, $Gd_2Zr_2O_7$ based coatings are thermally and chemically more stable at 1050 °C and thus they exhibit a better hot corrosion resistance than YSZ.

Whenever commercial or military aircraft fly over volcanoes and desert storms, the silica particles <80 μm attack the coating resulting in the formation of a glassy apatite phase that results in premature failure of the TBC components and this is referred to as Calcium Magnesium Alumino Silicate (CMAS) attack. The conventional YSZ readily dissolves in CMAS melt and hence there is a need to find alternative coatings. In general, the coatings with high optical basicity are less susceptible to CMAS attack. The promising CMAS resistant coatings are $Gd_2Zr_2O_7$ and $Y_3Al_5O_{12}$. The CMAS resistance of rare-earth zirconates against molten CMAS relies on the thermodynamics of the CaO-Ln_2O_3-SiO_2 system, where the solid $Ca_2Ln_8(SiO_4)_6O_2$ apatite phase is stable up to high temperatures (e.g., $Ca_2Gd_8(SiO_4)_6O_2$ is stable up to 1600 °C) and it also allows compositional variability over a relatively wide Ca/Ln ratio [46]. It indicates the initiation of CMAS and dissolution of rare-earth zirconate in the melt, the rare-earth cations secludes the main constituents of the molten phase (CaO and SiO_2), and solid apatite precipitates along the reaction interface, blocking further penetration [46-50].

Possible Replacements for YSZ

In order to overcome the hot corrosion and CMAS problems, rare earth pyrochlores are promising alternatives to YSZ [51]. However, the draw backs for pyrochlores is that there is no diffusion barrier to prevent reactions with the thermally grown oxide (TGO) and are characterized by a low toughness which results in a significant reduction in the erosion performance compared to standard 8YSZ. Therefore, multi-layered TBC such as 8YSZ/$Gd_2Zr_2O_7$ are promising. However, this coating will have lower erosion rate compared to $Gd_2Zr_2O_7$ while maintaining superior thermal conductivity over YSZ. Some of the promising

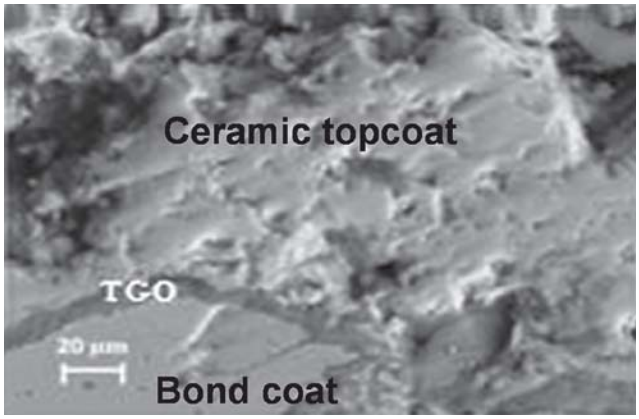

Fig. 12: Scanning electron micrograph of YSZ coating cross-section after 100 numbers of 1 hour thermal cycles at 1100°C.

ceramic materials such as $La_2Zr_2O_7$, $La_2Ce_2O_7$, $Gd_2Zr_2O_7$, $SrZrO_3$, $LaMgAl_{11}O_{19}$, $LaYbZr_2O_7$, $Yb_2Sn_2O_7$, $SrZrO_3$, $La(Mg_{1/4}Al_{1/2}Ta_{1/4})O_3$, Ba_2ErAlO_5, $Dy_2SrAl_2O_7$, $BaNd_2Ti_3O_{10}$, $LaPO_4$, etc., have also been explored.

Recent Trends in TBCs

To overcome the limitations of APS TBCs, suspension and solution precursor plasma spray processes have been explored. Studies have shown that suspension plasma spraying (SPS) technique is a propitious method for the fabrication of thermal barrier coatings (TBCs) with high porosity and good thermal shock resistance. This has been possible by realizing a feathery columnar structure[52].

Rare earth zirconates cannot be replaced for the conventional YSZ because of its mismatch with the TGO despite possessing lower thermal conductivity, lower CTE, lower sintering ability, and further it possesses lower fracture toughness than YSZ. Hence all the rare earth zirconates are combined with standard TBC YSZ to get multi-layered TBC architecture [53-57]. There is an interest in monitoring the failure patterns of the TBCs timely and dynamically using Finite Element Methods and the life prediction of the TBCs under the real service conditions[58].

TBC Developmental Activities at CSIR-NAL

At CSIR-NAL, plasma sprayable 8YSZ, doped YSZ , $La_2Ce_2O_7$, $Gd_2Zr_2O_7$, $La_2Zr_2O_7$ powders have been synthesized using cost-effective single step solution combustion method and co-precipitation methods and some of the processes have been patented[59-61]. The synthesized powders are mostly blocky angular in shape. To begin with, flowable zirconia powders doped with various mol% of yttria were prepared by the cost-effective and industrially viable chemical co-precipitation method[62]. The prepared powders were plasma sprayed using similar plasma spray parameters and the properties of the coatings were evaluated. Among them, plasma sprayed 3mol% yttria stabilized zirconia coating containing pure tetragonal zirconia exhibited highest wear resistance[62]. Later, plasma sprayable 8wt% YSZ powder was synthesized by the co-precipitation method without using any agglomeration step. This process has been patented in India and USA [59,60]. The indigenously developed 8 wt% YSZ powders possess very good flowability and particle size and hence were plasma sprayed on to the bondcoat which was deposited over a nickel superalloy substrate [63]. The coating showed a thermal conductivity of 0.80 W/mK vis-à-vis 0.70 W/mK exhibited by a plasma sprayed 8wt% YSZ coatingfrom a commercial powder. The rate of transformation of tetragonal zirconia to monoclinic zirconia was less in indigenous coating during the hot corrosion studies (Fig. 11). The coatings showed a porosity of ~19% and this was substantiated with mercury porosimeter data that showed 18% porosity. The coatings also showed thermal cycling capabilities at par with the commercial YSZ coating. The TGO thickness formed during thermal cycles was <10 μm.

Fine powder of CMAS with the composition of desert sand was prepared by solution combustion method (SCM) [64]. Flowable yttria-stabilized zirconia (YSZ) and cluster paired YSZ (/ doped with Dy-$_2$-O_3 and Gd_2O_3) powders synthesized by single-step SCM. The CMAS interaction with plasma sprayed TBCs was studied at 1200, 1270/ and 1340/ °C for 24/ h. TBC of cluster paired YSZ showed better CMAS resistance for doped YSZ-compared to YSZ coatings[64]. At CSIR-NAL, hot corrosion studies were carried out for plasma sprayed YSZ/$Gd_2Zr_2O_7$ and YSZ thermal barrier coating. The bi-layered coating showed improved hot corrosion resistance compared to YSZ [65]. YSZ/ $Gd_2Zr_2O_7$ bilayer TBC exhibited a higher thermal cyclic life (300/ cycles) than the single layer 8YSZ (175/ cycles) coatings at 1100/ °C.

Plasma sprayed $La_2Zr_2O_7$ (LZO) coating has been developed from LZO powders synthesized by SCM from urea as fuel in a single-step without using spray drying process[66]. The coating showed a thermal conductivity value of 1.08 $Wm^{-1}K^{-1}$ [66]. To overcome the limitations of the conventional YSZ TBCs, bilayered $La_2Ce_2O_7$ (LCO)/ YSZ[67] and LCO/cluster paired zirconia (gadolinia, dysprosia and yttria stabilized zirconia - (Gd,Dy,Y)SZ) plasma sprayed TBCs have been developed and their hot corrosion behaviour has been studied[67]. The study showed enhanced hot corrosion for LCO/(Gd,Dy,Y)SZ bilayered coating with 100 μm LCO thickness compared to LCO/YSZ system[68]. Attempts have also been made to develop metallic bond coat by electrolytic codeposition[69].

Conclusions

Thermal barrier coatings have become an integral part of GTs. Worldwide a lot of advances have been made with respect to the materials and coatings used for TBCs. There is a greater thrust to increase the turbine gas inlet temperatures to increase the efficiency of the GTs. To overcome the limitations of conventional YSZ, rare earth zirconates have been explored. Further to overcome the lower fracture toughness of rare earth zirconates, bilayered and multi-layered YSZ/rare earth zirconate coatings have

been explored. A lot of research work on different TBC ceramic topcoat materials is being pursued in various R & D organizations, academic institutes including CSIR-NAL.

Acknowledgements

The authors thank Director, CSIR-NAL and Head, SED for the encouragement. The authors also thank the financial assistance received from CSIR (HCP-0036). ❐

References

1. D.R. Clarke, M. Oechsner and N.P. Padture, *MRS Bull.* **37**, 891–898 (2012).
2. S. Bose and J. DeMasi-Marcin, *J. Therm. Spray Technol.* **6**, 99–104 (1997).
3. R.A. Miller, *J. Therm. Spray Technol.* **6,** 35–42 (1997).
4. U. Schulz, C. Leyens, K. Fritscher, M. Peters, B. Saruhan-Brings, O. Lavigne, J.M. Dorvaux, M. Poulain, R. Mévrel and M. Caliez, *Aerosp. Sci. Technol.* **7,** 73–80 (2003).
5. H. Herman, S. Sampath and R. McCune, *MRS Bull.* **25**,17–25 (2000).
6. J. H. Perepezko, *Science* **326,** 1068–1069 (2009).
7. R. Vaßen, M.O. Jarligo, T. Steinke, D.E. Mack and D. Stöver, *Surf. Coat. Technol.* **205**, 938–942 (2010).
8. N.P. Padture, *Science* **296**, 280–284 (2002).
9. P.G. Lashmi, P.V. Ananthapadmanabhan, G. Unnikrishnan and S.T. Aruna, *J. Eur. Ceram. Soc.* **40**, 2731-2745 (2020).
10. D. Zhu and R.A. Miller, *MRS Bull.* **25**, 43–47 (2000).
11. L. Liu, S. Wang, B. Zhang, G. Jiang, H. Liu, J. Yang, J. Wang and W. Liu, *J. Manuf. Process.* **97**, 12–34 (2023).
12. R. Darolia, *Int. Mater. Rev.* **6**, 315–348 (2013).
13. E. Bakan and R. Vaßen, *J. Therm. Spray Technol.* **26**, 992–1010 (2017).
14. L. Guo, W.T. He, W.B. Chen, Z.L. Xue, J. He, Y.Q. Guo, Y. Wu, L.H. Gao, D.Q. Li, Z. Zhang, L.L. Wei, Y.Y. Gao, T.H. Zhang, J. Qiao, Q.H. Li and H.B. Guo, *Surf. Sci. Technol.* **1**, 6 (2023).
15. R.A. Miller, *NASA/TM* 2009 - 215459 (2009).
16. W.N. Harrison, D.G. Moore and J.C. Richmond, *NACA TN-1186, National Advisory Committee for Aeronautics* (1947).
17. C.R. Morse, *NACA Research Memo E8120* (1948).
18. A.V. Levy, *Met. Prog.* **75**, 86–89 (1959).
19. L.N. Hjelm and B.R. Bomhorst, *NASA Tech Memo X-57072*, 227–253 (1961).
20. A.N. Curren, S.G. Grisaffe and K.C. Wycoff, *NASA TM X-2461* (1972).
21. SG Grisaffe, *Mach. Des.* **39**, 174–181 (1967).
22. G.W. Goward. *Proceedings of the workshop on coatings for advanced heat engines*, Castine, Maine, July 27-30, Washington DC, Department of Atomic Energy (1987).
23. S. Stecura, *NASA TM X-3425* and C.H. Liebert, F.S. Stepka, *NASA TM X-3352* (1976).
24. W.R. Sevdk and B.L. Stoner, *NASA Contractor Report CR-135360*, (Pratt & Whitney Aircraft) (1978).
25. S. Stecura, *NASA TM-78976* (1978).
26. S. Stecura, *Thin Solid Films*, **150,** 15–40 (1987).
27. N.P. Anderson and K.D. Sheffler, *Tasks I-III, NASA-CR-168251, PWA-5777-29* (1983).
28. P.A. Siemens and W.B. Hilg, *NASA CE-165351* (1981).
29. R.A. Miller, *NASA Tech Memo 87288* (1986).
30. R.A. Miller, *NASA Tech Memo* 79205 (1979).
31. S. Manning Meler and D.K. Gupta, *J. Eng. Gas Turbines Power*, **116**, 250–257 (1994).
32. R.A. Miller, *J. Eng. Gas Turbines Power 109*, 448–451 (1987).
33. N. Guglielmi, *J. Electrochem. Soc.* **119**, 1009–1012 (1972).
34. L.Z. Zhang, B.L. Bates and Y. Zhang, *Surf. Eng.* **33,** 136–141(2017).
35. F. Walsh and C. Ponce de León, *Trans. IMF.* **92,** 83–98 (2014).
36. W.R. Chen, X. Wu, B.R. Marple, D.R. Nagy and P.C. Patnaik, *Surf. Coat. Technol.* **202** 2677–2683 (2008).
37. S. Lokachari, K. Leng, A. R. Romero, N. Curry, G. Brewster, A. Norton and T. Hussain, *ACS Appl. Mater. Interface* **16**, 10646–10660 (2024).
38. R. Vaßen, Y. Kagawa, R. Subramanian, P. Zombo and D. Zhu, *MRS Bull.* **37**, 911–916 (2012).
39. V. Kumar and K. Balasubramanian, *Prog. Org. Coat.* **90**, 54–82 (2016).
40. G. Mehboob, M.-J. Liu, T. Xu, S. Hussain, G. Mehboob and A. Tahir, *Ceram. Int.* **46**, 8497–8521 (2020).
41. K. Xiong, J. Wang, X. Jin, C. Hou, W. Zhang, T. Hua and X. Fan, *Surf. Coat. Technol.* **478,** 130439 (2024).
42. W. Fan and Y. Bai, *Ceram. Int.* **42**, 14299–14312 (2016).
43. A. Pakseresht, F. Sharifianjazi, A. Esmaeilkhanian, L. Bazli, M.R. Nafchi, M. Bazli and K. Kirubaharan, *Mater. Des.* **22,** 111044 **(**2022).
44. Z. Yang, C. Luo, X. Zan, J. Zhang, W. Liu and W. Wang, *Surf. Coat. Technol.* **473** 129947 (2023).
45. M. Habibi, L. Wang and S.M. Guo, *J. Eur. Ceram. Soc.* **32**, 1635–1642 (2012).
46. S. Morelli, S. Bursich, V. Testa, G. Bolelli, A. Miccichè, L. Lusvarghi, *Surf. Coat Technol.* **439**, 128433 (2022).
47. M. Sigaroodi, J. Rahimi, E. Poursaeidi and F. Montakhabi, *Corro. Sci.* **227,** 111742, (2024).
48. H. Zhang, Y.Chen, L. Li, D. Yang, X. Liu, A. Huang, X. Zhang, J. Lu and X. Zhao, *J. Eur. Ceram. Soc.* **44**, 5154–5165 (2024).
49. H. Zhang, Y.Chen, L. Li, D.Yang, X. Liu, A. Huang, X. Zhang, J. Lu and X. Zhao, J. *Eur. Ceram. Soc.* **90**, 54-82 (2016).
50. M.K. Hossain, M.H.K. Rubel, Md.A. Akbar et al. *Ceram. Int.* **48**, 32588-32612 (2022).
51. L. Guo, B. Zhang, Q. He, M. Liu and L. Liang, *Surf. Coat. Technol.* **479,** 130523 (2024).
52. M. Mathanbabu, D. Thirumalaikumarasamy, P. Thirumal, M. Ashokkumar, *Mater. Today: Proc.* **46**, 7948-7954 (2021).
53. X. Liu, P. Zhang, Y. Lu, G. Liu, J. Sun, W. Liu, W. Pan and C. Wan, *Surf. Coat. Technol.* **471**, 129928 (2023).

54. K. Praveen, G. Shanmugavelayutham, D.S. Rao and G. Sivakumar, *Surf. Coat. Technol*. **465**, 129588 (2023).

55. X. Lu, J. Yuan, G. Li et al., *J. Eur. Ceram. Soc.* **44**, 5138–5153 (2024).

56. A. H. Esmaeilkhanian, F. Sharifianjazi, E. Ahmadi et al., *Mater. Today Commun.* **37,** 107514 (2023).

57. L. Wang, D.C. Li, J.S. Yang, F. Shao, X.H. Zhong, H.Y. Zhao, K. Yang, S.Y. Tao and Y. Wang, *J. Eur. Ceram. Soc.* **36(6),** 1313-1331(2016).

58. S.T. Aruna, N. Balaji and K.S. Rajam, IN284897, 2017.

59. S.T. Aruna, N. Balaji and K.S. Rajam, US 8546284B2, 2013.

60. S.T. Aruna, P.G. Lashmi and N. Balaji, IN404639, 2022.

61. S.T. Aruna, N. Balaji and K.S. Rajam, *Mater. Charact.* **62**, 697-705 (2011).

62. S.T. Aruna, B.A. Paligan, N. Balaji and V. P. Kumar, *Ceram. Int*. 4**0,** 11157-11162 (2014).

63. P.G. Lashmi, N. Balaji, K.A. Kumar, P.V. Ananthapadmanabhan, G. Unnikrishnan, S.S. Kumar and S.T. Aruna, *Ceram. Int.* **15,** 18255-1826445 (2019).

64. P.G. Lashmi, S. Majithia, V. Shwetha, N. Balaji and S.T. Aruna, *Mater. Charact.* **147,** 199-206 (2019).

65. S.T. Aruna, C. Sanjeeviraja, N. Balaji and N.T. Manikandanath, *Surf. Coat Technol.* **219,** 131-138 (2013),

66. P.G. Lashmi, P.V. Ananthapadmanabhan, Y. Chakravarthy, G. Unnikrishnan, N. Balaji, and S.T. Aruna, *J. Alloys Compd.* 711 (2017) 355-364.

67. P.G. Lashmi, N. Balaji, S.S. Kumar and S.T. Aruna, *Surf. Coat. Technol.* **409**, 126901 (2021).

68. M. Srivastava, J.N. Balaraju, B. Ravisankar and V.K.W. Grips, *Appl Surf. Sci.*, 263, 597–607 (2012).